

Electron paramagnetic resonance applications: promising developments at the E K Zavoisky Kazan Physical-Technical Institute of the Russian Academy of Sciences

K M Salikhov

DOI: 10.3367/UFNe.2016.02.037760

Contents

1. Introduction	588
2. Electron paramagnetic resonance in materials science	588
3. Search for molecular magnets	589
4. Spatial arrangement of paramagnetic centers ('architecture' of spin labels)	589
5. Hyperpolarization of electron spins in the course of spin-dependent photoinduced processes	590
6. Spin exchange in diluted solutions of paramagnetic particles	592
7. Quest for systems and realization of quantum logical operations with the use of electron spins as qubits	593
8. Conclusion	594
References	594

Abstract. This paper briefly reviews the advances made in recent years at the E K Zavoisky Kazan Physical-Technical Institute of the Russian Academy of Sciences in EPR spectroscopy and its applications to overcoming the topical problems.

Keywords: electron spin, electron paramagnetic resonance, spin hyperpolarization, qubits, bimolecular collisions

1. Introduction

Electron paramagnetic resonance (EPR) (spin resonance) was discovered by E K Zavoisky in Kazan in 1944. During the time since its discovery, the EPR method has turned into one of the most informative techniques for studying the molecular electronic structure, structural defects, color centers in crystals, dynamic properties of condensed matter, mechanisms of chemical reactions, and the structure and mobility of biomolecules. EPR enjoys wide use in materials science, dosimetry, and medicine, in particular, for monitoring the content of oxygen and nitrogen oxide (NO) in the human body, monitoring the quality of food products, dating archaeological finds, etc. Modern EPR techniques permit developing new technologies, for instance, controlling spin-

dependent chemical reactions and spin-dependent recombination luminescence, open up possibilities for quantum calculations involving electron spins as qubits, etc. Owing to the development of pulsed multifrequency and high-frequency techniques, EPR spectroscopy provides unique data about the molecular mechanisms of biological processes, specifically about the mechanism of solar energy assimilation by photosynthetic systems. EPR finds increasingly wide application in the structural investigation of disordered systems, which is especially important in the study of living systems. It is hardly possible to enumerate the areas where EPR is applied, they are numerous, and new proposals are steadily emerging. The present is seeing the true Renaissance of EPR spectroscopy.

EPR spectroscopy is developing along a variety of lines at the E K Zavoisky Kazan Physical-Technical Institute (KPTI) of the Kazan Scientific Center of the Russian Academy of Sciences. EPR is employed to study solid-state laser materials, spin clusters for molecular magnets and memory elements, the nonequilibrium hyperpolarization of electron spins arising from spin-dependent elementary photoinduced processes, etc. Also developed are EPR tomography and quantum calculations built around electron spins.

The intention of this paper is to present the selected significant results recently obtained at KPTI using a variety of EPR techniques.

2. Electron paramagnetic resonance in materials science

Among the traditional areas of work at KPTI is the EPR investigation of materials for quantum electronics, solid-state lasers, the study of the structural, magnetic, and optical properties of paramagnetic centers formed by the impurity

K M Salikhov E K Zavoisky Kazan Physical-Technical Institute,
Kazan Scientific Center of the Russian Academy of Sciences,
ul. Sibirskii trakt 10/7, 420029 Kazan, Russian Federation
E-mail: kevsalikhov@mail.ru

Received 4 February 2016

Uspekhi Fizicheskikh Nauk 186 (6) 659–666 (2016)

DOI: 10.3367/UFNr.2016.02.037760

Translated by E N Ragozin; edited by A Radzig

ions of transition group elements in dielectric crystals, and the determination of spin energy levels. In recent years, it was revealed with the help of EPR spectroscopy that in a number of cases paramagnetic centers in laser crystals exhibit a tendency to associate. In synthetic forsterite Mg_2SiO_4 , the concentration of pairs of two closely located impurity ions, Cr^{3+} , Ho^{3+} , Tb^{3+} , and Er^{3+} , was shown to be several orders of magnitude higher than the number of such pairs expected for a random Poisson distribution [1, 2]. It turned out that such self-organization of dimers in forsterite is not observed for Tm^{3+} ions.

3. Search for molecular magnets

Another traditional line of KPTI research is the development of EPR spectroscopy of spin clusters. Initially, this research was primarily aimed at elucidating the properties of exchange interaction between the ions of transition group elements and the influence of different factors on the sign and magnitude of the exchange integral and the anisotropy of this interaction. This information is possible to obtain by way of detailed theoretical analysis of the shape of EPR spectra.

At present, this research places an emphasis on the search for spin clusters which might serve as monomolecular magnets to be used as magnetic molecular sensors or for information storage and processing [3]. The relevance of this quest is due to the fact that monomolecular magnets may, in principle, be employed as qubits in quantum computers. Of special interest are clusters with dysprosium ions Dy^{3+} , which exhibit a large anisotropy of magnetic properties. Despite the fact that EPR may yield direct information about the anisotropy of local magnetic properties of Dy ions and the character of spin–spin interaction in clusters, EPR research on these systems is practically nonexistent. As far as we know, the first EPR investigation of clusters with dysprosium ions possessing monomolecular properties was performed at KPTI [3].

4. Spatial arrangement of paramagnetic centers ('architecture' of spin labels)

The spatial arrangement of paramagnetic centers (PCs) in solids is important for radiation chemistry, photochemistry, quantum electronics, the implementation of quantum calculations with the use of electron spins as qubits, etc. The addressed implantation of spin labels into protein molecules opens up the possibility of making preselected spin architectures. Detailed information about the spatial distribution of these spin labels is helpful, for instance, in the determination of the structure of proteins which do not lend themselves to crystallization.

The distance between PCs and their mutual arrangement in space determine the magnitude of dipole–dipole (DD) spin–spin interaction between the PCs. Therefore, the mutual arrangement of the PCs may be determined if there is a way to measure the DD interaction parameter. This can be done by EPR spectroscopy techniques.

Recording the effect of DD interaction between the PCs in EPR experiments is not quite a trivial task. Indeed, in many cases the DD interaction scale for the PCs in solids is several orders of magnitude smaller than the scale of hyperfine interaction with magnetic nuclei, and the spread of Zeeman frequencies of PC electron spins due to g -tensor anisotropy and/or the nonuniformity of an external magnetic field.

Under these conditions, it is extremely hard to extract the contribution of the DD interaction to the electron spin dynamics against the background of other contributions if use is made of stationary EPR spectroscopy techniques. Assistance is rendered by pulsed EPR spectroscopy techniques.

Pulsed EPR techniques, which are based on the observation of electron spin-echo signals, permit getting rid of the masking effect of inhomogeneous broadening of resonance frequencies and extracting directly the contribution of the relatively weak DD interaction. For instance, when microwave (MW) pulses, which form the signal of the so-called primary electron-spin echo, excite both partners in a pair of paramagnetic particles, the echo-signal amplitude $V(2\tau) = V_0 \cos(D_{AB}\tau)$ oscillates at a frequency which corresponds to the DD interaction energy D_{AB} (here, τ is the time interval between the two MW pulses that form the primary electron-spin echo signal).

Pulsed EPR spectroscopy has become at present the most important method of investigating the spatial PC distribution in solids. A major impetus to the progress in this field was provided by the development of a double (two-frequency) pulsed EPR method (double electron–electron resonance, DEER). This method was first proposed and experimentally realized for determining the interpartner distance distribution function for the pairs of free radicals produced in photolysis [4]. A three-pulse protocol of the experiment was proposed in the latter work [4]. According to this protocol, $\pi/2$ and π MW pulses, the first and third pulses of the protocol, are applied at the resonance frequency ω_A of A type spins at the points in time $t = 0$ and $t = \tau$. These pulses form the experimentally observed spin-echo signal at the point in time $t = 2\tau$. A π MW pulse is additionally applied at the resonance frequency ω_B of B type spins at the point in time $t = T$. In the experiment, τ is fixed, while T is varied in the interval $(0, \tau)$.

In this situation, the observed signal is described by the expression [4]

$$V(T, \tau) = V_0(1 - p_B + p_B \cos(D_{AB}T)), \quad (1)$$

where V_0 is the signal amplitude without MW pumping, p_B is the probability of the B spin inversion by the MW pump pulse at the instant $t = T$, and D_{AB} is the DD interaction parameter; for a paramagnetic center with an isotropic g -factor, this parameter takes the form

$$D_{AB} = \frac{g_A g_B \beta^2 (1 - 3 \cos^2 \theta) / r_{AB}^3}{\hbar} \equiv D_{0AB} (1 - 3 \cos^2 \theta),$$

$$H_{d-d} = \hbar D_{AB} S_{Az} S_{Bz}.$$

Here, r_{AB} is the distance between A and B, and θ is the angle between vector \mathbf{r}_{AB} and the direction of the external magnetic field.

Equation (1) has come into wide use in DEER research for determining the separation of paramagnetic labels in biological molecules, even in situations when the applicability conditions of Eqn (1) are known to be violated. The derivation of Eqn (1) relies on the assumption that none of the microwave pulses excites both partners of the pair in a DEER experiment. This becomes possible when the partners of the PC pair possess entirely different resonance frequencies and the EPR spectra of the partners do not overlap. In practice, however, in the majority of cases both partners of

the pair are nitroxyl radicals, so that the EPR spectra of spin labels in the pair decidedly overlap or even coincide. This signifies that each of the microwave pulses in a DEER experiment may, to one degree or another, excite both partners of the pair, and therefore Eqn (1) may not be used to interpret the data of DEER experiments.

In recent papers [5, 6], we generalized the theory of three- and four-pulse protocols of DEER experiments for systems of paramagnetic particles with overlapping EPR spectra. The theory was developed for the case when the EPR spectrum width is by far greater than the difference between the carrier frequencies of the microwave pulses that excite the DEER signal. For the three-pulse experiment protocol, the contribution to the observed signal made by the spins A of AB pairs is given by the expression

$$V(T, \tau) = V_0 [(1 - p_A)(1 - p_B) + p_A(1 - p_B) \cos(D_{AB}\tau) + p_B(1 - p_A) \cos(D_{AB}T)] + p_A p_B \cos[D_{AB}(\tau - T)]. \quad (2)$$

In formulas (1) and (2), p_B are the same, and p_A is the probability of B-spin inversion by a microwave pulse at the point in time $t = \tau$. The contribution from spins B of AB pairs to the observed signal is described by expression (2) if the subscripts are transposed, $A \leftrightarrow B$. It should be noted that Eqn (2) goes over into Eqn (1) if the partner of the spin under consideration in the pair is not excited by the pulse at the point in time $t = \tau$, i.e., $p_A = 0$.

By comparing formulas (1) and (2), one can see that the overlapping of EPR spectra and spin label excitation spectra gives rise to new terms in the observed signal. In practice, along with the three-pulse DEER experiment protocol, use is made of a four-pulse protocol, in which case, as in the three-pulse protocol, the signal observed for a pair of spins contains only one term dependent on the time intervals between the pulses, provided the EPR spectra of the spins in the pair do not overlap. When these spectra overlap, in general, six additional terms appear [6]. The additional terms do not contain new modulation frequencies in the signal observed in DEER experiments, but they have different phases and may significantly change the amplitude of the observed signal and the depth of its modulation, which is formed as the sum of several contributions. These additional terms rise in importance with an increase in the number of spin labels in clusters. Their inclusion, therefore, becomes indispensable when the DEER method is employed for determining the ‘architecture’ of the spatial arrangement of three or more spin labels and, in particular, for determining the number of spin labels in such clusters.

To test the theory, we undertook an experimental investigation of the behavior of the DEER signal for biradicals. Figure 1 plots the experimental data for one of the biradicals. Also shown there are the results of numerical calculations according to Eqn (1), ignoring the overlap of the EPR spectra of the spins in a pair, and according to Eqn (2), i.e., with the inclusion of the real overlap of these spectra.

Figure 1 suggests that a better agreement between theoretical and experimental data is possible to achieve with Eqn (2). The distance between the radical centers was calculated from the modulation frequency of the observed signal. It turned out to be equal to 1.7 nm.

The DEER theory was generalized [5, 6] to the case of clusters containing three or more paramagnetic particles. A theoretical expression was derived for the spin-echo signal in

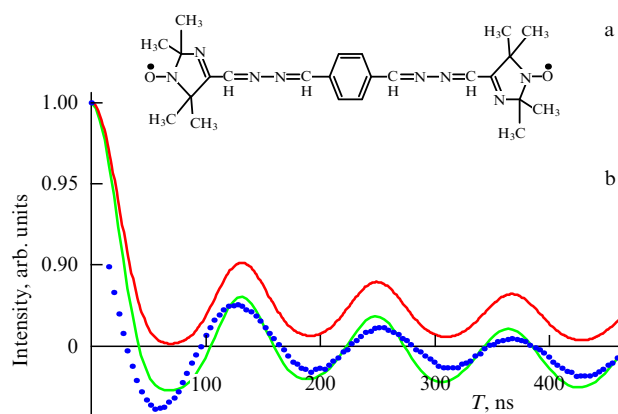


Figure 1. (a) Structural formula of the biradical investigated. (b) DEER signal intensity as a function of time interval T between the first and second microwave pulses. Dots stand for experimental data. Solid curves show the results of calculations with Eqn (1) (upper curve) and Eqn (2) (lower curve).

the three- and four-pulse versions of DEER experiments for the clusters of paramagnetic centers, when the EPR spectra of the paramagnetic centers overlap, including the instance of polyradicals containing the same nitroxyl radicals.

The topicality of this work is due to the following fact. For spin labels in the investigation of the structure of biomacromolecules in biological applications of DEER, use is made of nitroxyl radicals with strongly overlapping (or even coinciding) EPR spectra.

The DEER experiments based on utilization of nitroxyl radicals as spin labels permit measuring distances between PCs in the range of ≈ 1.5 –8 nm. This estimate may be obtained from the following considerations. For distances between PCs shorter than 1.5 nm, the DD interaction interferes with the relatively strong exchange interaction, which hampers marking out the DD interaction and determining the distance between the PCs. For nitroxyl radicals, the decay of spin-echo signals occurs in a time on the order of 1 μ s. For the signal modulation to have time to manifest itself, the modulation frequency must exceed several megahertz. This condition yields an estimate of about 8–10 nm for the distances which may be measured in DEER experiments.

5. Hyperpolarization of electron spins in the course of spin-dependent photoinduced processes

Spin-dependent processes are currently attracting considerable interest. Examples are provided by the recombination of free radicals, intramolecular radiationless intercombination transitions, etc. In recent decades, EPR was shown to possess great potentialities as a tool for investigating these processes. This is due to the following circumstances. Participating in spin-dependent processes are unpaired electrons, paramagnetic particles. And so the EPR effect, EPR spectroscopy techniques may be employed for their investigation. Elementary spin-dependent molecular acts proceed not infrequently on a nanosecond time scale. Modern time-resolved and pulsed EPR spectroscopy techniques permit real-time observations of electron spin dynamics down to the nanosecond time scale. Observations of the EPR effect in the course of

spin-dependent processes permit obtaining unique information and showing up their mechanism in detail. The study of spin-dependent processes, in turn, has lent a powerful impetus to the further development of the EPR spectroscopy itself. The point is that electron spins in the course of spin-dependent processes find themselves in such nonequilibrium states that would be difficult, if not impossible, to prepare if the elementary processes did not obey certain spin selection rules.

By way of example, let us consider the photoionization of molecules in a condensed medium. In the majority of cases, the ground molecular electronic state possesses the total electron spin $S = 0$. The photoionization is induced by an electric dipole transition, and therefore the spin state of electrons is conserved in this elementary act. Consequently, immediately after the photoionization of molecule M , an ion M^+ forms with one unpaired electron and an electron. Therefore, two paramagnetic particles emerge and, on the face of it, it is possible to observe the EPR effect. But this pair of paramagnetic particles, each of which has an electron spin $S = 1/2$, is produced in the singlet state with the total zero spin, and it should not be observed in an EPR experiment. If the spin dynamics in the pair can change the spin multiplicity, for instance, singlet–triplet transitions may occur in this example, then the EPR effect may be observed. Notice that the signal intensity in the EPR experiment will oscillate in the example considered above.

Photoinduced spin hyperpolarization results from certain spin selection rules in elementary molecular processes which ‘prepare’ electron spins in a correlated (coherent) state, and the subsequent spin dynamics during which the dipole spin polarization observed in experiments forms. To illustrate, we briefly mention the main formation stages of electron spin hyperpolarization in the framework of the triplet polarization mechanism.

In the absorption of light quantum, molecules pass from the singlet ground electronic state S_0 to an electronic excited singlet state S_1 . Next, the spin–orbit interaction induces a radiationless intramolecular singlet–triplet transition to an excited triplet state T . The singlet–triplet transitions caused by spin–orbit coupling are selective, and triplet spin states T_x , T_y , and T_z are unequally populated. Let P_x , P_y , and P_z denote the population probabilities of the respective triplet eigenstates T_x , T_y , and T_z in a zero magnetic field. However, under conditions whereby the spin–orbit interaction is much stronger than the Zeeman interaction, it may be assumed that the triplet molecules in an external magnetic field are also produced in the initial state which is described in the T_x , T_y , and T_z function basis by the density matrix

$$\rho_T(0) = \{ \{P_x, 0, 0\}, \{0, P_y, 0\}, \{0, 0, P_z\} \}. \quad (3)$$

For this density matrix, the average values S_x , S_y , and S_z are equal to zero, i.e., the triplet molecules appear in the state with a zero spin dipole moment. However, triplet molecules are produced in the state with a nonzero spin quadrupole moment. Specifically, for state (3) we have

$$\begin{aligned} Q_{xy} &= \langle S_x^2 - S_y^2 \rangle = P_y - P_x, \\ Q_{zz} &= \left\langle S_z^2 - \frac{S(S+1)}{3} \right\rangle = \frac{P_x + P_y - 2P_z}{3}. \end{aligned} \quad (4)$$

The spin Hamiltonian of the molecule in a triplet state may be represented as the sum of the Zeeman interaction H_Z and the

interelectron spin–spin interaction H_{ss} :

$$H_T = H_Z + H_{ss}, \quad H_Z = \beta \mathbf{S} \mathbf{g} \mathbf{B}, \quad H_{ss} = \mathbf{S} \mathbf{D} \mathbf{S}, \quad (5)$$

where β is the electron magneton, g is the spectroscopic splitting tensor, and D is the splitting tensor of the triplet spin states in a zero magnetic field. In the system of principal axes of the tensor D , spin Hamiltonian H_{ss} may be represented as

$$H_{ss} = D \left(S_z^2 - \frac{S(S+1)}{3} \right) + E(S_x^2 - S_y^2). \quad (6)$$

Spin Hamiltonian (5) does not commute with the quadrupole and dipole moment tensor components. That is why the quadrupole moment changes as a result of spin dynamics, and a spin dipole moment simultaneously appears. The appearance of the dipole moment is easily calculated for a relatively short time [7]. We apply the temporal perturbation theory to conclude that the dipole moment appears in the second order in time. By averaging over all possible spatial orientations of the triplet molecule, we obtain the average value of the spin dipole hyperpolarization of the triplet molecule:

$$\begin{aligned} M(T) &= \frac{1}{3} g B_0 [3E(P_y - P_x) + D(P_x + P_y - 2P_z)] \frac{t^2}{\hbar^2} \\ &= \frac{1}{3} g B_0 (3EQ_{xy} + DQ_{zz}) \frac{t^2}{\hbar^2}. \end{aligned} \quad (7)$$

It can be seen from Eqn (7) that the spin dipole polarization of the molecule in a triplet state contains two terms, which are proportional to the initial values of the two spin quadrupole moment components of the triplet molecule, Q_{xy} and Q_{zz} defined by Eqn (4).

At present, we are investigating the photoinduced nonequilibrium hyperpolarization of electron spins in supramolecules based on metal porphyrin complexes. Porphyrins show great promise from the standpoint of synthesizing new functional materials. Porphyrin compounds with paramagnetic ion complexes permit obtaining materials with prescribed magnetic properties.

In Ref. [7], an investigation was made of the spin dynamics of the photoexcited state of the system of a zinc porphyrin molecule covalently bound to a copper complex, ZnPCu. The echo-detected EPR protocol is as follows. A microwave pulse is applied, which inverts magnetization. In the course of subsequent relaxation to the equilibrium value, the magnetization of the system passes through zero. A laser pulse is applied at this instant, which gives rise to nonequilibrium spin polarization. Immediately after the termination of the laser pulse, two microwave pulses are applied to form a spin-echo signal for observing the nonequilibrium spin polarization. This protocol makes it possible to directly observe the photoinduced spin polarization.

The experimental data obtained by time-resolved EPR spectroscopy (Fig. 2) and the echo-detected EPR technique suggest that the electron spins of ZnPCu subunits—the photoexcited triplet zinc porphyrin (spin $S = 1$) and the copper ion (spin $S = 1/2$)—are indicative of nonequilibrium hyperpolarization. This observation testifies to the existence of spin–spin interaction between these two subunits. The shape of EPR spectra and the data of echo-detected nutation spectroscopy suggest that this spin–spin interaction is weaker than that in triplet excited porphyrin. It is possible

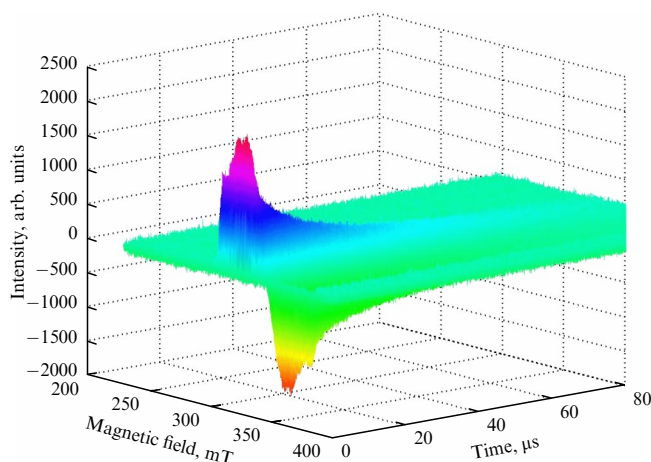


Figure 2. Time-resolved two-dimensional EPR spectrum of the ZnPCu system at a temperature of 40 K after photoexcitation.

to interpret the experimental data under the assumption that the spins of triplet zinc porphyrin are hyperpolarized by the triplet mechanism, and the spins of copper ions are polarized due to the transfer of the polarization from triplet zinc porphyrin as a result of spin exchange induced by the exchange interaction.

Simulations of the EPR spectrum of the zinc porphyrin triplet excited state have shown that good agreement with experiment may be achieved if the following values of the parameters are put: $D = 1100$ MHz, $E = 157$ MHz, $P_x = 0.15$, $P_y = 0$, and $P_z = 0.85$. Substitution of these parameters into Eqn (7) gives $M(T) < 0$, which corresponds to the positive effect of integral spin polarization of excited triplet porphyrin, which is observed in EPR spectra. The experiment allows conclusion that the EPR spectrum of copper ions also manifests the effect of positive integral spin polarization of copper ions. This observation testifies that the transfer of spin polarization from porphyrin to a copper ion in the system under study is induced by exchange rather than dipole–dipole interaction. From experimental data, it follows that the magnitude of integral spin polarization of porphyrin exceeds the integral polarization of a copper ion. This observation suggests that the exchange interaction between porphyrin and the copper ion is relatively weak. At the same time, the exchange interaction should be stronger than the dipole–dipole interaction between the porphyrin and copper ion spins. Based on this reasoning, we estimate the exchange integral at $J \sim 10^8$ MHz.

6. Spin exchange in diluted solutions of paramagnetic particles

Biomolecular processes play a significant part in chemical kinetics, catalysis, etc. Among the biomolecular processes is a spin exchange—the mutual spin flip of the unpaired electrons of two paramagnetic particles upon their collision. The spin exchange is of interest by itself, but in the majority of cases it serves as a model process for determining the collision frequency and the rate constant of biomolecular reactions.

Modern EPR spectroscopy techniques permit determining the rate of this biomolecular process with a high accuracy, because spin exchange is responsible for the concentration line broadening in EPR spectra and the shift of line positions,

transforms symmetrically shaped EPR spectrum components to asymmetric ones, etc. These characteristic shape variations of EPR spectra permit determining the frequency of spin exchange in quite different systems, even, for instance, in such complex ones as the cells of living organisms. Spin exchange is a relatively simple biomolecular process, and the construction of a detailed theory is therefore possible. There is a rather well-elaborated theory for calculating the rate constant for the spin exchange between uncharged paramagnetic particles. Spin exchange is extensively used in molecular biology. To illustrate the application of spin exchange theory, mention should be made of the study of accessibility of active ferment portions to low-molecular substrates. To this end, it is possible to selectively attach a spin label to the ferment structure and add a spin probe to the system. By analyzing the shape variation of the spin-label EPR spectrum upon increasing the spin probe concentration, it is possible to obtain useful information about the rate constant of spin exchange and eventually about the accessibility of active ferment portions to the substrates.

In biological systems, we are also dealing with charged particles, which makes the theoretical analysis of spin exchange at the pairwise collisions of charged paramagnetic particles relevant. Coulomb interaction refers to a long-range one, and therefore it is impermissible to take into account the interaction of two particles at only the instants of time of their close approach, even for very low particle concentrations. However, the situation is radically different when consideration is made of charged paramagnetic particles (spin probes) in electrolytes. Owing to Debye screening, the interaction of two charges in electrolytes acquires a short-range nature: the hyperbolic dependence of the interaction potential on the distance r between charges, $U \sim 1/r$, is replaced with the exponentially decreasing dependence $U \sim (1/r) \exp(-r/r_D)$, where r_D is the Debye screening radius. That is why there is good reason to develop the theory of pair collisions in electrolytes for sufficiently low concentrations of charged spin probes.

We formulated the kinetic equations for single-particle spin density matrices for charged spin probes in electrolytes with the inclusion of their pairwise collisions. The contribution of pairwise collisions is expressed in terms of the pair encounter efficiency operator P for spin probes; the equations were developed for doing calculations P [8].

Let us consider a system with a spin Hamiltonian $H = \sum_k H(k) + \sum_{n,k} H(k,n)$, where $H(k)$ is the spin Hamiltonian of the k th particle, and $H(k,n) = J_0 \exp[-\kappa(r - r_0)] \mathbf{S}_k \mathbf{S}_n$, where r_0 is the shortest interparticle distance at a collision, \mathbf{S}_k is the spin moment operator of the k th particle, and κ defines the steepness of the exchange integral decrease with an increase in interparticle distance. The kinetic equation for a single-particle spin density matrix has the form

$$\frac{\partial \rho_1(1)}{\partial t} = -\frac{i}{\hbar} [H(1), \rho_1(1)] - C \text{Tr}_2 P \rho_1(1) \rho_1(2),$$

$$P = \int W(r) G(r) d^3 \mathbf{r}.$$

Here, the superoperator $W(r)$ is determined by exchange interaction:

$$W(r) = \frac{i}{\hbar} J(r) [(\mathbf{S}_1 \mathbf{S}_2) \times E - E \times (\mathbf{S}_1 \mathbf{S}_2)],$$

$$J(r) = J_0 \exp[-\kappa(r - r_0)],$$

and E is the unit operator in the space of two spins.

The superoperator $G(r)$ is found from the solution of the boundary-value problem:

$$L(r)G(r) + W(r)G(r) + [Q_0, G(r)] = 0,$$

$$Q_0 = \frac{i}{\hbar}(H_0 \times E - E \times H_0), \quad H_0 = H(1) + H(2).$$

The operator $L(r)$ describes the divergence of the flux of the partial spin density matrix for the subensemble of spin probe pairs at a given distance \mathbf{r} between them. This flux is made up of the diffusion flux and the drift of spin probes caused by the Coulomb interaction potential:

$$L(r)\rho_2(\mathbf{r}) \equiv -\operatorname{div} \mathbf{j}(\mathbf{r}),$$

$$\mathbf{j}(\mathbf{r}) = -D \operatorname{grad} \rho_2(\mathbf{r}) - \frac{D}{kT} \rho_2(\mathbf{r}) \operatorname{grad} U(\mathbf{r}),$$

$$U(\mathbf{r}) = \frac{q_1 q_2}{\varepsilon r} \exp\left(-\frac{r}{r_D}\right).$$

In these equations, D is the mutual diffusion coefficient of two spin probes, and q_1 and q_2 are the charges of colliding spin probes. The equation for $G(\mathbf{r})$ must be solved for the boundary conditions: $\lim_{r \rightarrow \infty} G(\mathbf{r}) \rightarrow E$ according to the correlation relaxation principle ($\rho_2(r_{12}, t) \rightarrow \rho_1(t)\rho_1(t)$, $r_{12} \rightarrow \infty$), and at the distance of closest approach of the spin probes it is necessary that $j(r_0) = 0$.

A difference scheme was derived and an efficient calculation algorithm was developed for the numerical solution of the above equations. Using these mathematical tools, we made numerical calculations of the rate constants of bimolecular spin exchange reactions between similarly and oppositely charged paramagnetic particles in solutions for a large set of parameters of exchange interaction, permittivities, Debye screening radii, and spin probe diffusion coefficients.

The results of calculations allow the following conclusions.

- The effective spin-exchange radius shortens with an increase in the mutual diffusion coefficient. On the strength of this dependence of the effective spin exchange radius on the diffusion coefficient, the spin exchange rate constant $K_{\text{ex}} = 4\pi R_{\text{eff}} D$ ceases to be a linear function of the particles' mutual diffusion coefficient D . The shortening of the effective radius with an increase in the mutual diffusion coefficient takes place due to the shortening of the residence time of two colliding particles in the domain of efficient exchange interaction.

- The effective spin-exchange radius depends on the steepness of a decrease in the exchange interaction potential. The effective particle residence time depends not only on the diffusion coefficient, but also on the steepness of the exchange integral decrease with an increase in interparticle distance. The steeper the decrease in the exchange integral, the smaller the domain of efficient interaction and, as a result, the smaller the effective spin-exchange radius.

- If the effective spin-exchange radius exceeds the half-radius of closest approach, a situation of strong spin exchange takes place. In the case of oppositely charged particles, the Coulomb attraction provides a sufficiently long time for particle residence in the interaction domain, which is why, for oppositely charged radicals, as a rule, a situation of strong exchange occurs. In this case, the effective spin-exchange radius increases logarithmically in relation to the magnitude of the exchange integral at a distance of the closest approach of the radicals.

- For a sufficiently large coefficient of mutual particle diffusion and sufficiently large steepness of a decrease in the

exchange integral, the spin exchange interaction ceases to be strong even for the collisions of oppositely charged particles.

Therefore, we have developed for the first time a consistent theory of bimolecular spin exchange in the solutions of charged paramagnetic particles in electrolytes with allowance made for the extended nature of the exchange interaction. A program was constructed for the numerical calculation of the spin exchange rate constant. The full-fledged theory was employed to analyze experimental data on concentration line broadening in the EPR spectrum of charged spin probes. Exchange interaction parameters were determined by comparing the data found in experiments and simulations.

7. Quest for systems and realization of quantum logical operations with the use of electron spins as qubits

We are working on the implementation of quantum logical operations with the use of electron spins in paramagnetic centers as qubits [9, 10]. Organic biradicals may be successful candidates for the role of a two-qubit system, which is required, for instance, for realizing the basic logical Control-NOT (CNOT) operation. However, the existence of two qubits is a necessary but not sufficient condition for one biradical or another to be really usable in the implementation of quantum logical operations. To do this, the biradicals must possess certain properties.

First, the electron spins in a biradical must be characterized by sufficiently long decoherence times. We believe that these times should not be shorter than several microseconds, and should at least markedly exceed 100 ns. Otherwise, it will be impossible to realize CNOT type logical operations prior to the onset of decoherence of electron spin states. According to our theoretical analysis, to realize CNOT with electron spins requires more than 20 microwave pulses, which takes a time interval of about 200 ns [9].

Second, the magnitude of spin-spin interaction between two radical centers in a biradical should lie within certain limits. The spin-spin interaction should not be too weak; otherwise, it will not manage to form spin coherence in the pair of spins. But this interaction should not be too strong, either; otherwise, serious problems will emerge with spin-selective (addressed) excitation of individual electron spins by microwave pulses in the course of implementation of logical operations for electron spins.

At this stage of project execution, we are studying the properties of different biradicals in the quest for systems that could be used in quantum computing. We are determining the spin decoherence times with the aid of the electron spin-echo technique. For instance, a decrease in the signal of the so-called primary spin echo (the echo-signal formed by two short microwave pulses) is a direct way to measure the time of irreversible spin decoherence. The shape of EPR spectra in stationary experiments and the behavior of signals observed in pulsed EPR experiments permit the magnitude of spin-spin interactions between radical centers in biradicals to be determined with a sufficiently high accuracy. In the search for biradicals suited for the realization of CNOT, we investigated the magnetic resonance and relaxation parameters of the biradicals attached to C_{60} fullerenes and biradicals based on lanthanide beta-diketonate complexes (Fig. 3).

So far, we have not found a system among the investigated biradicals that satisfied all requirements imposed on a pair of

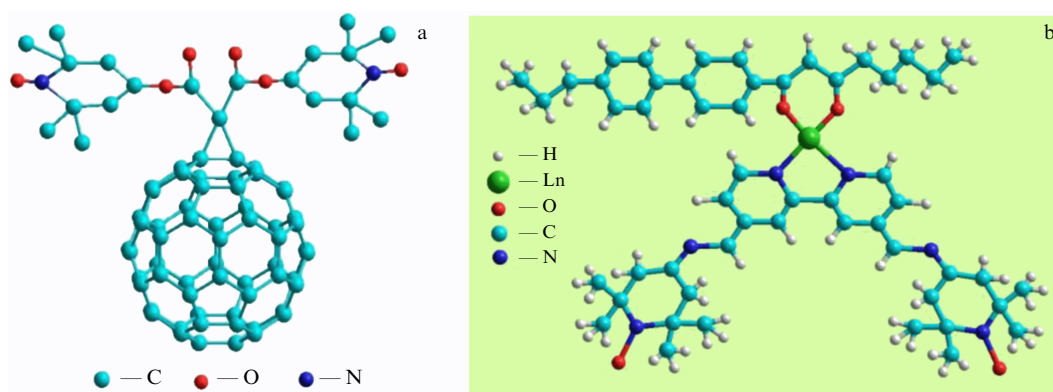


Figure 3. (a) Examined C_{60} systems with one attached biradical. (b) Biradicals synthesized on the base of lanthanide beta-diketonates complexes.

qubits for the realization of quantum logical CNOT operation.

The quantum coherence of qubits is central to quantum computing. Several mechanisms are responsible for the coherence relaxation of electron spins utilized as qubits. In Ref. [10], we showed that the relaxation of electron spin coherence due to hyperfine interaction may be controlled using a sequence of microwave pulses.

By way of example, we considered the pulse sequence exploited in Carr–Purcell experiments. It was shown both theoretically and experimentally that the spin coherence relaxation slows down with an increase in the number of π pulses in the Carr–Purcell sequence. This observation is reminiscent of the so-called quantum Zeno paradox, which involves measurements of the state of a quantum system slowing down quantum computing (quantum dynamics). The more often a quantum system is subject to measurements, the slower the quantum evolution. The microwave field pulses in the Carr–Purcell experiment protocol perform a unitary transformation (rotation) of the spin state, and so they may not be identified with the measurement in which the spin state is projected onto a certain state. At the same time, these pulses of the external electromagnetic field are responsible for the formation of spin-echo signals which are observed (measured) in experiments. Thus, these pulses may be viewed as a part of the measurement procedure.

It is also noteworthy that we consider the microwave field in the framework of classical physics, and the measuring instruments in quantum mechanics must be classical. With the above considerations in mind, we believe that in experiments with the Carr–Purcell protocol the moderation of electron spin dephasing due to spectral diffusion, which is caused by the hyperfine interaction of the electron spins with the magnetic nuclei of the matrix, may phenomenologically be treated as a kind of ‘quantum Zeno effect’. We note that the observed moderation of spin phase relaxation in the Carr–Purcell experiment may also be treated as a manifestation of the averaging of electron spin interaction with magnetic nuclei, effected by microwave pulses. However, from the standpoint of the prospect of quantum computing with electron spins, it is highly instructive to treat the moderation of spin phase relaxation due to the spectral diffusion, which emerges in the Carr–Purcell experiment as a peculiar manifestation of the quantum Zeno effect.

The manifestation of the quantum Zeno effect in the Carr–Purcell experiment protocol gives grounds to anticipate that this effect may show up also in other protocols

involving microwave pulse sequences. For example, it was shown in Ref. [9] that the implementation of the logical quantum CNOT operation invites the application of a long sequence of microwave pulses. Proceeding from the above data and reasoning, we expect that the contribution of magnetic nuclei to electron spin dephasing (decoherence) in the CNOT implementation with electron spins may be decreased owing to the quantum Zeno effect. We plan to investigate this effect in the near future. The Zeno effect in multipulse experiment protocols under discussion may also be employed for error corrections in the realization of quantum computing.

8. Conclusion

The above examples of EPR spectroscopy application suggest that EPR has great potential for the solution of scientific problems in physics, chemistry, and molecular biology, as well as for laying the scientific foundation for spin technologies, and that the E K Zavoisky Kazan Physical-Technical Institute is making a considerable contribution to the progress of EPR spectroscopy and its applications.

Acknowledgments

The author wishes to express his deep gratitude to the colleagues V K Voronkova, R T Galeev, R B Zaripov, A E Mambetov, A A Sukhanov, and V F Tarasov for their cooperation. This study is supported by the State Program and the Program of Basic Research of the Presidium of the Russian Academy of Sciences.

References

1. Tarasov V F et al., in *Modern Development of Magnetic Resonance 2015, Kazan, Russian Federation, September 22–26, Abstracts of the Intern. Conf.* (Ed. K. M Salikhov) (Kazan: Zavoisky Physical-Technical Institute, 2015) p. 138
2. Konovalov A A et al. *Appl. Magn. Reson.* **45** 193 (2014)
3. Baniodeh A et al. *Dalton Trans.* **42** 8926 (2013)
4. Milov A D, Salikhov K M, Shirov M D *Sov. Phys. Solid State* **23** 565 (1981); *Fiz. Tverd. Tela* **23** 975 (1981)
5. Salikhov K M, Khairuzhdinov I T, Zaripov R B *Appl. Magn. Reson.* **45** 573 (2014)
6. Salikhov K M, Khairuzhdinov I T *Appl. Magn. Reson.* **46** 67 (2015)
7. Sukhanov A A et al. *Appl. Magn. Reson.* **46** 1199 (2015)
8. Salikhov K M et al. *Appl. Magn. Reson.* **45** 911 (2014)
9. Volkov M Yu, Salikhov K M *Appl. Magn. Reson.* **41** 145 (2011)
10. Zaripov R et al. *Phys. Rev. B* **88** 094418 (2013)